Energy Proceedings
Vol 36, 2023
ISSN 2004-2965

Thickening Characteristics of methane hydrate film in Gas-liquid Interface

Hui Zhang[1,2,3], Jing-Chun Feng[1,2,3*], Yongming Shen[1,2,3], Bin Wang[1,2], Yan Xie[1,2], Yue Zhang[1,2], Li Tang[1,2]

1 School of Ecology, Environment and Resources, Guangdong University of Technology, Guangzhou, 510006, P. R. China.
2 Southern Marine Science and Engineering Guangdong Laboratory (Guangzhou), Guangzhou, 511458, P. R. China.
3 Guangdong Provincial Key Laboratory of Water Quality Improvement and Ecological Restoration for Watersheds, Institute of Environmental and Ecological Engineering, Guangdong University of Technology, Guangzhou, 510006, China.

ABSTRACT

The kinetic law of natural gas hydrate (NGH) growth is highly significant for the application of NGH technology. In this work, we observed the process of methane hydrate film thickening at the gas-liquid interface by X-ray Computed Tomography (X-CT). Our results showed that the methane hydrate film growth process at the gas-liquid interface can be divided into three stages. Firstly, the methane hydrate film formation process was controlled by heat transfer; secondly, the thickening process was controlled by mass transfer. Above all, the transport of water below the hydrate film caused fractures in the hydrate film, and new hydrate grows at the fractures. The proposed hydrate film formation and growth mechanism at the gas-liquid interface in this study provided theoretical support and research methodology for future studies of the gas-liquid interface growth process of NGH.

Keywords: natural gas hydrate, hydrate film, X-ray CT, mass transfer control, heat transfer control

1. INTRODUCTION

Marine sediments is the largest reservoir of methane [1], which is not only a promising clean energy source but also a greenhouse gas 20 times more potent than carbon dioxide in terms of its greenhouse effect [2, 3]. Methane hydrates in marine sediments are stable under certain temperature and pressure conditions. However, once natural gas hydrates dissociate or dissolve due to pressure fluctuations, temperature changes, or changes in chemical composition, methane gas bubbles or methane-rich fluids can migrate upward into the seabed and water column. Temperature changes caused by global warming and variations in hydrostatic pressure (such as changes in sea level) may exacerbate the instability of hydrates [4, 5]. If the stored methane in marine sediments escapes into the atmosphere, it can have disastrous consequences for the climate [6].

Marine methane sinks play a significant role in preventing methane from entering the atmosphere, especially in deep-sea seabed environments, where they absorb a large amount of methane leakage from the seafloor. The formation of methane hydrates is a specific process for capturing and sequestering freely migrating methane emissions from the seafloor. The upward release of gaseous methane from sediments forms methane hydrates in sediment pores or fractures at certain temperature and pressure conditions, effectively sequestering methane on the seabed.

The phenomenon of hydrocarbon seepage in marine sediments is widespread along continental margins [7]. Hydrocarbons migrate from the sediment upwards, creating unique natural phenomena like gas plumes, and forming special ecological zones such as hydrothermal vents and cold seeps [8, 9]. The speed of gas migration in nature is not constant; some regions have high flow rates, leading to the formation of large gas plumes on the seafloor [10], while in other regions, flow rates are low, making it difficult to observe significant gas plumes. During the upward migration of gas through porous media, specific migration channels are formed, and under appropriate conditions, solid methane hydrates are generated. The formation and distribution characteristics of these migration channels are closely related to the speed of gas migration.

Currently, there is limited research on the movement of bubbles during dynamic bubbling processes, as capturing dynamic processes can be challenging. Optical microscopes are commonly used to

This is a paper for the 9th Applied Energy Symposium: Low Carbon Cities and Urban Energy Systems (CUE2023), Sep. 2-7, 2023, Matsue & Tokyo, Japan.

study hydrate formation on bubbles. For instance, Li et al. [11] simulated the rise of hydrate gas bubbles in deep water and observed the rupture of hydrate films and secondary growth along cracks in the hydrate films. Zeng et al. [12] used in-situ Raman techniques to study the morphology of hydrate films and mass transfer channels during the thickening and growth of hydrates on bubbles. However, these studies are based on bubbles suspended in water. Research on the movement of bubbles in porous media is even scarcer. Opaque porous media can hinder optical microscope observations of bubbles. Currently, there is limited attention on the fate of methane bubbles under different seepage scenarios in porous media, especially regarding the formation of methane hydrates under in-situ seafloor conditions.

In order to investigate the formation characteristics of gas migration channels during the upward migration of gas in porous media and the distribution characteristics of methane hydrate formation, we used non-destructive X-CT to study the evolution of migration channels and the distribution of hydrate formation during gas migration processes. We propose mechanisms for the evolution of migration channels under different flow rates.

2. MATEIAL AND METHODS

2.1 Apparatus

The growth characteristics of NGH under specific conditions were observed using X-CT in conjunction with a hydrate synthesis unit, as shown in Fig. 1. X-CT detects the internal structure of samples through the differences of attenuation coefficients. The equipment consists of an x-ray source, an x-ray detector and a data acquisition system. Hydrate synthesis unit consists of a sample chamber, pressurization system and data acquisition system. The sample chamber consists of a reactor and cooling system. The reactor can withstand a maximum pressure of 15 MPa and a minimum temperature of −2°C, which meets the conditions for the formation of NGH. The temperature is monitored and regulated by thermocouples with a measuring error of ±0.1°C. The pressure sensor is used to test the reactor pressure. The high-pressure reactor is located on a rotating/moving platform for X-CT detection during hydrate formation under target pressure and temperature conditions.

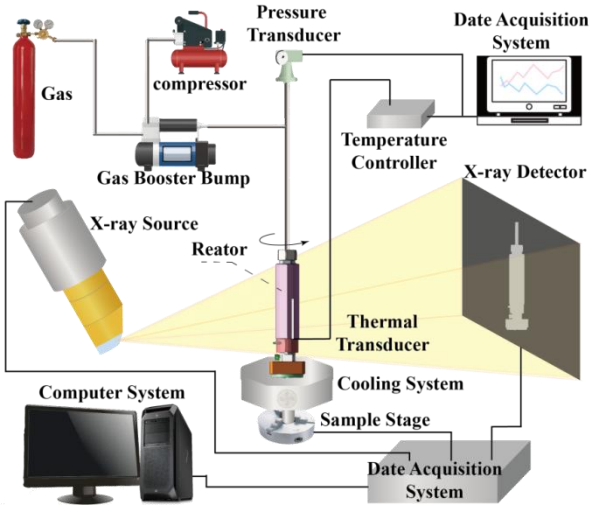

Fig. 1. The combined experimental system of the X-CT equipment and a hydrate synthesis unit.

2.2 Materials

Experimental materials include methane gas (99.9% pure, China Guangzhou Yuejia gas Co., LTD) and brine for NGH formation. 5 wt% KI solution was prepared using KI (Aladdin) and ultra-pure water. KI used in this study were reagent grade and were supplied by Aladdin (Shanghai, China). Ultra-pure water (18.2 mΩ·cm^{-1}) used in this study was prepared by a Millipore water system (ELGA Purelab Chorus PC1LSCXM2, UK). Brine is used instead of pure water for the following reasons: first, the density of the aqueous solution is similar to the density of NGH, and the denser brine is used in order to enhance the contrast of the image; second, a large amount of methane is stored in the marine environment, and brine is close to seawater in nature which is better able to show the growth characteristics of hydrates in the ocean.

2.3 Experimental procedures

Before the experiment, the reactor was cleaned with ultra-pure water for three times. And then it was purged with nitrogen to avoid impurities, while 3.5 mL of KI solution was slowly injected into the reactor. After that methane was injected into the reactor until the experimental pressure was reached and stabilized for 8 h to fully dissolve the methane into the solution. The reactor temperature was then reduced to the target temperature to induce hydrate formation. The time at which the temperature reached the experimental condition was set to time 0, and CT scans were subsequently performed at different intervals to obtain the spatial distribution and morphological characteristics of the hydrate. The hydrate generation experiments were carried out at 2°C under the pressure conditions of 10 MPa and 12 MPa, respectively.

3. RESULTS AND DISCUSSION

3.1 *Identification and extraction process of hydrate membrane at gas-water interface.*

In order to obtain information about the internal structure of the gas hydrate samples in the reactor, the scanned digital slices were reconstructed into three-dimensional bodies by a reconstruction algorithm in VG Studio. At the same time, median filtering was used to remove the noise from the original image and to differentiate between the different components (gas, water, and gas hydrate) based on the gray value. The hydrate portion was extracted separately for wall thickness analysis using VG Studio. The overall process is shown in Fig 2.

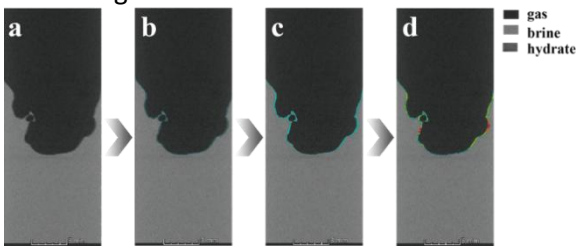

Fig. 2. Identification and extraction process of hydrate membrane at gas-water interface. (a) Initial image; (b) After thresholding; (c) Hydrate film region extraction; (d) Performing thickness analysis.

3.2 *Apparatus Mechanisms of hydrate film growth at the gas-liquid interface*

The gas-liquid interface hydrate generation experiments were carried out at 10 MPa and 12 MPa, respectively. And the change process of the hydrate film was constantly monitored using CT. The processed experimental results are shown in Fig. 3.

Firstly, it can be observed that under both experimental conditions, NGH first grew as a film at the gas-liquid interface. The rate of hydrate film formation varied under different pressures. The higher pressure caused a faster film formation. Due to the limitation of the resolution of the equipment, the initial hydrate film was too thin to be detected. Only when the hydrate film formed a certain thickness (more than 20 μm) can it be effectively detected, hence the initial film formation process was difficult to be observed. The experiment took the formation of a certain thickness of hydrate film as the initial point. An observable hydrate film can be formed at the gas-liquid interface in 2 h under the pressure of 12 MPa, while it took about 22 h to form an observable hydrate film at the gas-liquid interface under 10 MPa pressure.

The hydrate film was not uniformly thickened over time, but locally thicker, which was observed under different pressure tests. Immediately afterwards, the local thickened part began to undergo concave deformation below the liquid surface, while the thickness of the hydrate film in the concave part was not uniform. The concave deformation continued in the thick part of the hydrate film. And the cycle continued, finally forming a concave and uneven hydrate film which is like a string of bubbles bulging below the liquid surface. It was also found that when the NGH was highly concave, a large amount of hydrate could be detected on the wall and top of the reactor, as shown in Fig. 3c. This indicated that a more significant wall-climbing effect occurred in the later stage of hydrate growth.

According to the experimental phenomenon, it was presumed that the NGH in the reactor first grew as a film at the gas-liquid interface. Then, the water under the liquid surface was transported upward along the reactor wall due to the capillary force to form a new gas-liquid interface on the reactor wall. The new gas-liquid interface hydrate grew rapidly under the hydrate-stabilized condition. At this point, the loss of water below the hydrate film liquid surface caused the hydrate film to deform and form fractures, which can be observed in the 10 MPa and 24 h. The presence of the fractures caused further contact between gas and water, and continued the rapid formation of hydrate at the fractures. Resulting in the growth of unusual hydrate objects, similar to gas bubbles, from the hydrate film in the aqueous phased at the fractures. With the continuous upward transportation of water, new fractures were continuously generated at the gas-liquid interface. A special hydrate with a concave shape grew at the gas-liquid interface. The special hydrate object wall was hydrate membrane, hydrate membrane on the upper side of the methane, the lower side of the solution. Equivalent to the new gas-liquid interface hydrate membrane, the process continued to cycle, ultimately leading to the gas-liquid interface hydrate membrane was constantly concave. A large number of NGH was formation in the reaction kettle wall. It was worth noting that throughout the experiment, the hydrate film did not keep thickening, but continued to grow by generating fractures. The thickness of the hydrate film remained around 40 μm in most areas throughout the process. The initial fractures generation, on the contrary, produced the thickest hydrate film in the whole process, which was about 150 μm.

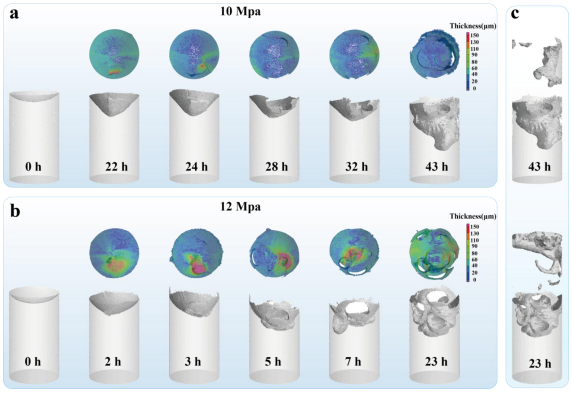

Fig. 3 Hydrate film growth process with different pressures. (a) 10 MPa; (b) 12 MPa; (c) hydrate wall climbing effect under two pressures, 10 MPa above and 12 MPa below.

We used VG Studio to extract and calculate the volume of hydrate film at the gas-liquid interface, while the results are shown in Fig. 4. Under the pressure conditions of 12 MPa and 10 MPa, the volume of hydrate film after film formation was 3.34 cm^3 and 5.87 cm^3, respectively. Under the two different pressure conditions, the volume of hydrate film did not change much for a period of time after the formation of hydrate film. When the hydrate membrane continued to grow and the degree of hydrate membrane deformation was high, the volume of hydrate membrane increased.

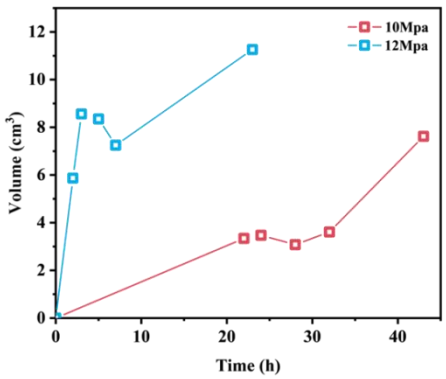

Fig. 4. Volume of Hydrate film change at the gas-liquid interface.

The possible formation mechanism of the hydrate film was conjectured as follows: after the rapid formation of the hydrate film at the gas-liquid interface, the growth of the hydrate film was changed from heat-transfer control to mass-transfer control. At this time, due to the capillary force, the liquid under the liquid surface was transported upward, resulting in the pressure difference between two sides of the hydrate film to form fractures or other defects. The formation of this defect provided a ternary contact line along between gas, solution and hydrate. This contact promoted the overgrowth of the free surface of the hydrate membrane. Because of the flexibility of the hydrate membrane and the constant pressure difference between two sides of the membrane, the newly formed hydrate membrane grew in the form of a depression. The mechanical strength of the new hydrate membrane was weaker than that of the earlier formed hydrate membrane. Therefore, the change kept occurring on the newly formed hydrate membrane, which also led to the eventual formation of a concave hydrate membrane that grew in the form of a bubble string.

A similar phenomenon was observed by Andrey S. Stoporev et al [13]. They attributed this to the effects of the indicated active agent. However, we observed the phenomenon without surfactant. We further verified the mechanism by using CT as the means of observation to obtain variations in the thickness distribution across the hydrate film.

4. CONCLUSIONS

The investigation of NGH formation processes at the gas-liquid interface is crucial for the application of hydrate technology, especially for the development of NGH resources and carbon sequestration processes in the ocean. This study provided experimental evidence for the growth process of gas hydrate at the gas-liquid interface. The structural changes of the hydrate film growth process at the gas-liquid interface were detected by X-CT scanning. The experimental results showed that the hydrate film at the gas-liquid interface did not grow by uniform thickening, and the hydrate film grew continuously at fractures under the pressure difference between the inside and outside of the hydrate film, which will eventually cause the hydrate grow into bubbles. This investigation on the growth of methane hydrate at the gas-liquid interface is of great significance to the study of the environmental and resource effects of NGH.

ACKNOWLEDGEMENT

The authors would like to acknowledge the financial support from the National Natural Science Foundation of China (42325603, 42022046, 42227803, 52122602, 41890850), the National Key Research and Development Program (2021YFF0502300), the Guangdong Natural Resources Foundation, (GDNRC[2022]45, GDNRC[2023]30), and the PI project of Southern Marine Science and Engineering Guangdong Laboratory (Guangzhou) (GML20190609 and GML2022009).

REFERENCE

[1] Piñero E, Marquardt M, Hensen C, Haeckel M, Wallmann K. Estimation of the global inventory of methane hydrates in marine sediments using transfer functions. Biogeosciences. 2013;10:959-75.

[2] Church J, Clark P, Cazenave A, Gregory J, Jevrejeva S, Levermann A, et al. Climate Change 2013: The Physical Science Basis. Contribution of Working Group I to the Fifth Assessment Report of the Intergovernmental Panel on Climate Change. Sea Level Change. 2013:1138-91.

[3] Knoblauch C, Beer C, Liebner S, Grigoriev MN, Pfeiffer EMJNCC. Methane production as key to the greenhouse gas budget of thawing permafrost. 2018;8:309-12.

[4] Biastoch A, Treude T, Rüpke LH, Riebesell U, Roth C, Burwicz EB, et al. Rising Arctic Ocean temperatures cause gas hydrate destabilization and ocean acidification. 2011;38.

[5] Knittel K, Boetius A. Anaerobic oxidation of methane: progress with an unknown process. Annual review of microbiology. 2009;63:311-34.

[6] Feng JC, Yan J, Wang Y, Yang Z, Zhang S, Liang S, et al. Methane mitigation: Learning from the natural marine environment. Innovation (Cambridge (Mass)). 2022;3:100297.

[7] Feng J-C, Wang Y, Li X-S, li G, Chen Z. Production behaviors and heat transfer characteristics of methane hydrate dissociation by depressurization in conjunction with warm water stimulation with dual horizontal wells. Energy. 2015;79.

[8] Suess E. Marine Cold Seeps: Background and Recent Advances. In: Wilkes H, editor. Hydrocarbons, Oils and Lipids: Diversity, Origin, Chemistry and Fate. Cham: Springer International Publishing; 2018. p. 1-21.

[9] Kurian PJ, Rajan S, Agarwal DK, Linsy P. Indian Ocean Ridge System and Seafloor Hydrothermal Activity. Journal of the Geological Society of India. 2022;98:155-64.

[10] Liu B, Chen J, Yang L, Duan M, Liu S, Guan Y, et al. Multi-beam and seismic investigations of the active Haima cold seeps, northwestern South China Sea. Acta Oceanologica Sinica. 2021;40:183-97.

[11] Li S-L, Sun C-Y, Chen G-J, Li Z-Y, Ma Q-L, Yang L-Y, et al. Measurements of hydrate film fracture under conditions simulating the rise of hydrated gas bubbles in deep water. Chemical Engineering Science. 2014;116:109-17.

[12] Xin-Yang Z, Wu G, Jiang W, Yang C, Meng Q, Chen G, et al. Effects of Inhibitors on the Morphology and Kinetics of Hydrate Growth on Surface of Bubble. Journal of Natural Gas Science and Engineering. 2019;74:103096.

[13] Stoporev AS, Adamova TP, Manakov AY. Insight into Hydrate Film Growth: Unusual Growth of Methane Hydrate Film at the Interface of Methane and the Aqueous Solution of Malonic Acid. Crystal Growth & Design. 2020;20:1927-34.